The red halo of Mrk 900 – a case study

Göran Olofsson 2008-01-17

Background

Extended red halos around different types of galaxies signal a population of low-mass stars with high mass/luminosity ratios and consequently contributing significantly to the mass of these galaxies. The low surface brightness of these haloes makes them, however, difficult to observe and the present case study is aiming at a careful investigation of the halo around Mrk 900, a blue, compact galaxy with several bright regions of star formations in the centre. The bright central region and the faint halo close to it means that the there is a clear risk that instrumental effects may introduce systematic errors in the determination of the surface brightness of the halo. If, for instance, the PSF (Point Spread Function) is less steep in the red than in the blue, then light from the central region may artificially redden the halo. In addition, the sky background is strongly increasing with background, which adds to the uncertainty in defining the surface brightness in the red region.

Observations

We used PolCor-2 on NOT for these test observations. This instrument is intended for coronagraphic imaging of polarized light near bright stars (such as debris disks), and for this reason it is constructed for high-contrast imaging. Thus, instead of using multi-element lens optics for the collimator and the camera (which is normally used in multi-purpose cameras for astronomy) PolCor-2 has two off-axis parabolic mirrors with extremely high reflectivity (>99.5%) from the UV to the CCD cut-off. The effect of diffraction off the 'spiders' (the support blades of the secondary mirror) is much reduced by a rotating, computer controlled, Lyot mask. Instead of a conventional CCD array, an EMCCD is used, allowing semi-simultaneous observations in the four polarizer positions (and, in addition, a *dark* monitoring). This camera also allows 'shift-and-add' and frame selection, which substantially improves the resulting sharpness. By removing the occulting disk of the coronagraph and the polarizer, PolCor-2 can be used for normal imaging with the advantage of being free from optical ghosts and the potential of producing high contrast images.

Mrk 900 was observed with PolCor-2 in two filters, Bessel-V and Bessel-I. These filters are relatively broad and their effective wavelengths in combination with the detector response function are around 530 nm and 850 nm respectively. The frame rate was 10 Hz and for each filter, 12000 frames were collected and some 15 % of these were rejected in the shift-and-add procedure. A similar number of frames were added to define the PSF, using a field star. The Mrk 900 observations were followed by a calibration on a Landolt standard star (SA113 221). Sky flat-fields were taken in the morning.

Technical aspects

a) PSF

For each radius around the PSF star, we calculate the median value (to avoid the effect of residual spider diffraction) and also the mean value (to get a clue to the *average* effect of the spider diffraction). It turned out that the mean and the median values differed by less than 1% and we can conclude that the average effect caused by the spiders is small. In Fig 1 we show the measured PSF for the two photometric bands. We also include the calculated PSF for a perfect telescope in space. The difference is two magnitudes and there are probably several contributions to the added brightness in

PSF wings (such as figuring errors of the telescope mirrors, dust scattering etc), but the result is still quite good.

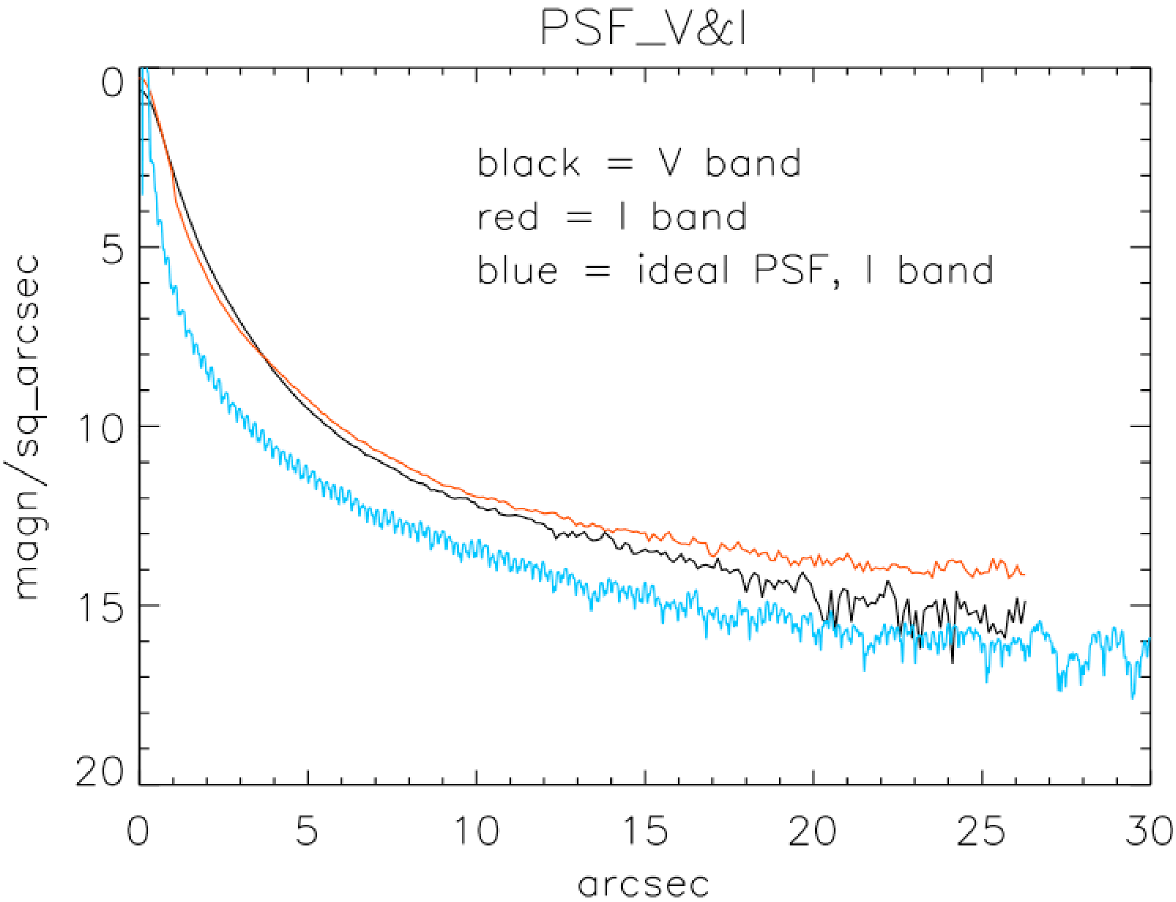

Fig 1. The observed PSF of PolCor-2 on the NOT. The ideal PSF for the I band is also shown.

b) Flat-field

The optics, including an under-sized Lyot stop, and a detector with a smooth response and a proper AR coating, result in quite nice Flat-fields. These are shown in Fig 2.

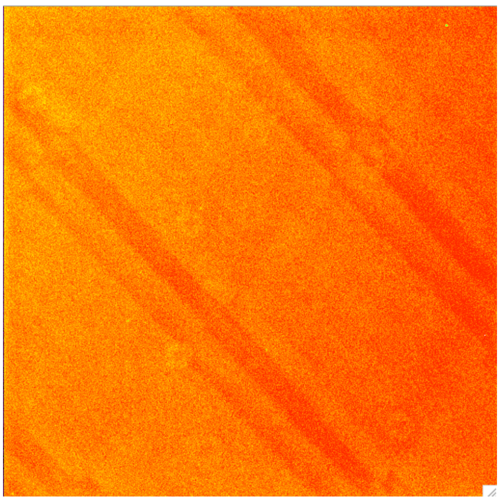

Fig 2a The Flat-field in V

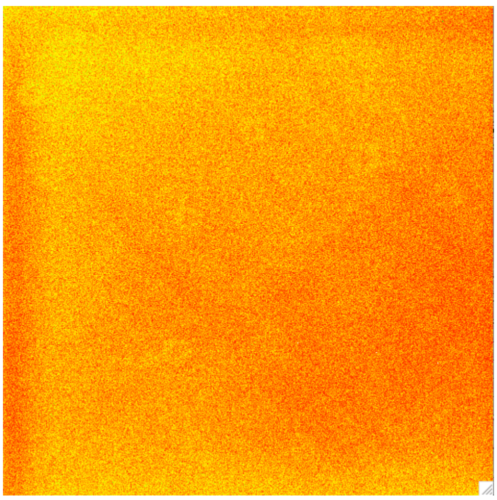

Fig 2b The Flat-field in I

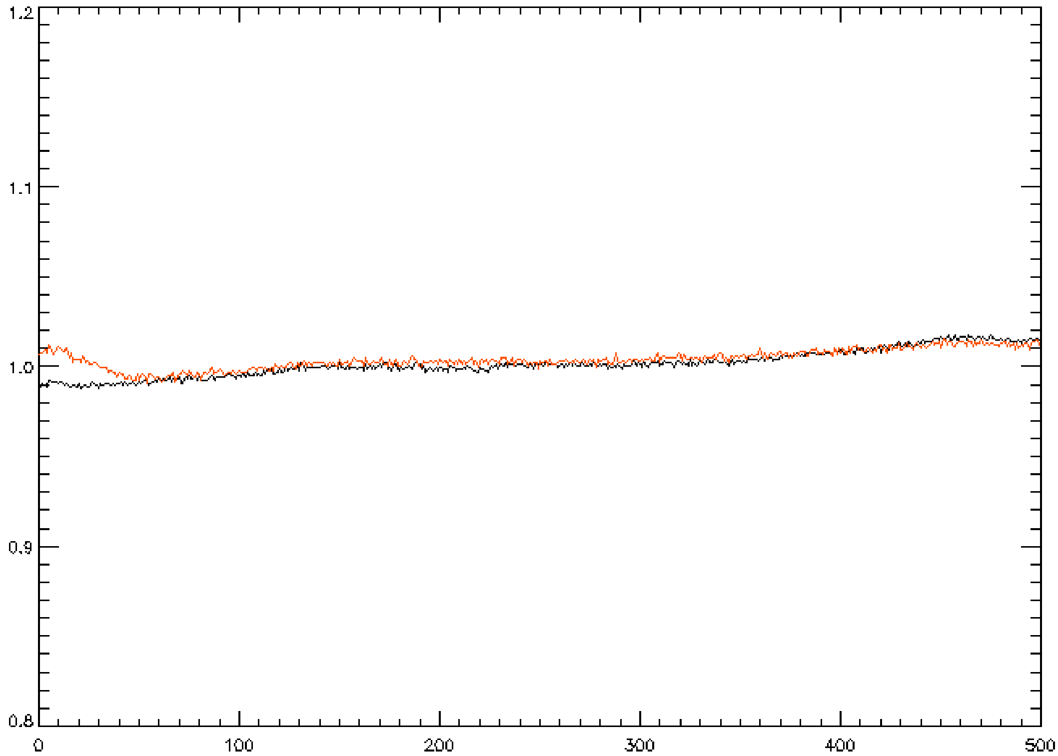

Fig 2c A cut across the Flat-fields (black is the V band and red is the I band). Note that there is no enhancement in the centre of the field (indicating that there is no contribution from scattered light off the sky baffles

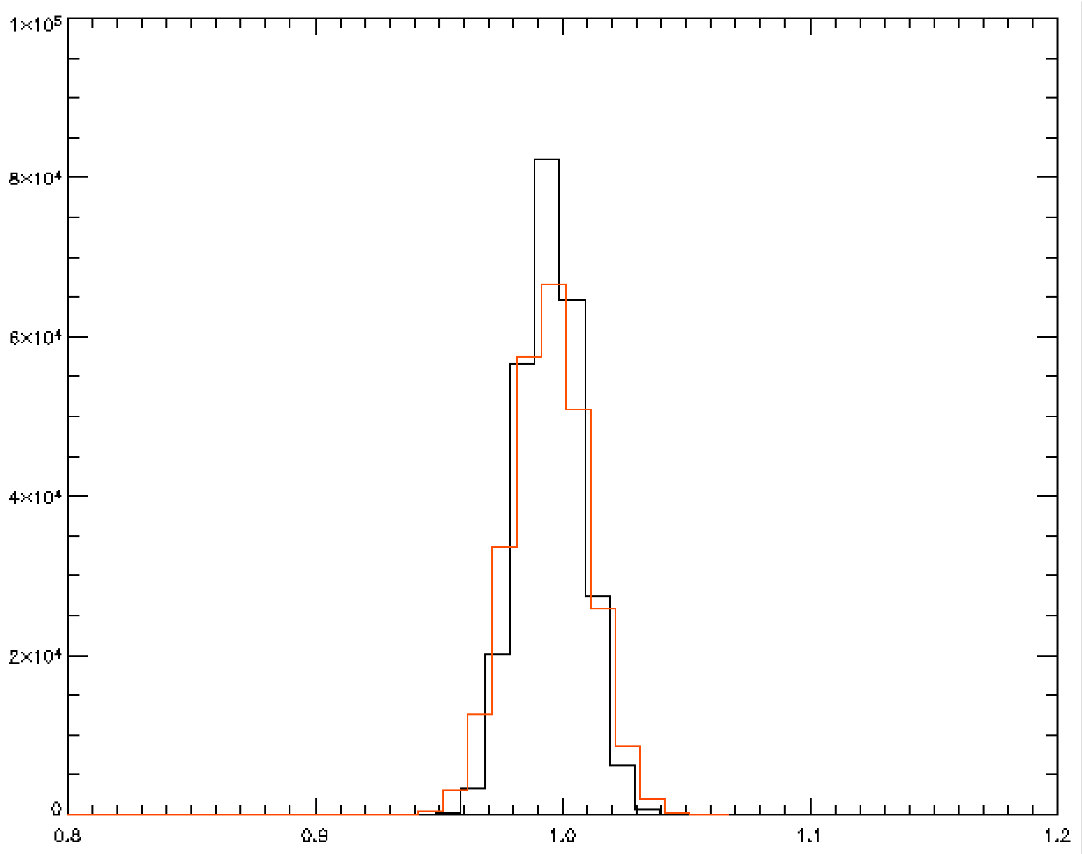

Fig 2d The pixel histograms of the FFs in V (black) and I (red). Note that > 99% of the pixels have values within +/- 3%.

c) The linearity.

Not much is known about the photometric quality of EMCCDs, and in particular it is important to take possible deviations from linearity into account. For this reason we have measured the linearity in the lab, and Fig 3 shows that it is in fact excellent.

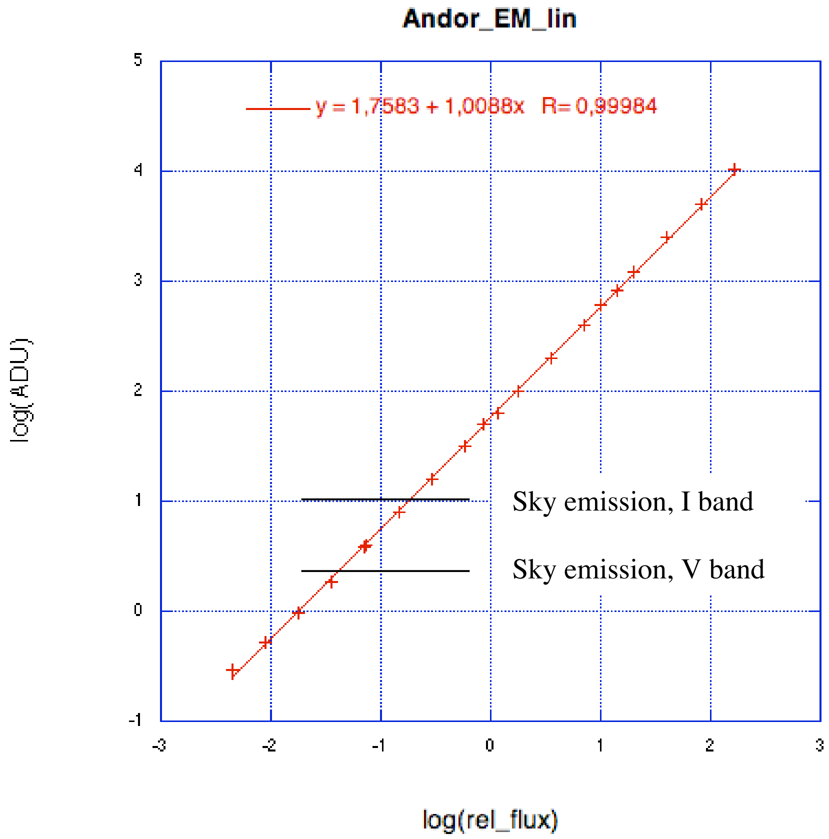

Fig 3 The Andor Ixon EMCCD camera has a linear response over five orders of magnitude. The gain parameter was set to 3200, corresponding to an EM gain of around 100.

d) The sky conditions

It is often difficult to judge from CCD images whether clouds have been in the line of sight during the observations, and with no moon, the available all-sky web cameras are generally not efficient in revealing cirrus clouds. The EMCCD techniques, however, makes it easy to monitor (or at least reconstruct) the sky transmission as well as the sky emission. In Fig 4 we show the sky transmission and emission in the V and I bands during the observations of Mrk 900. This also applies for the

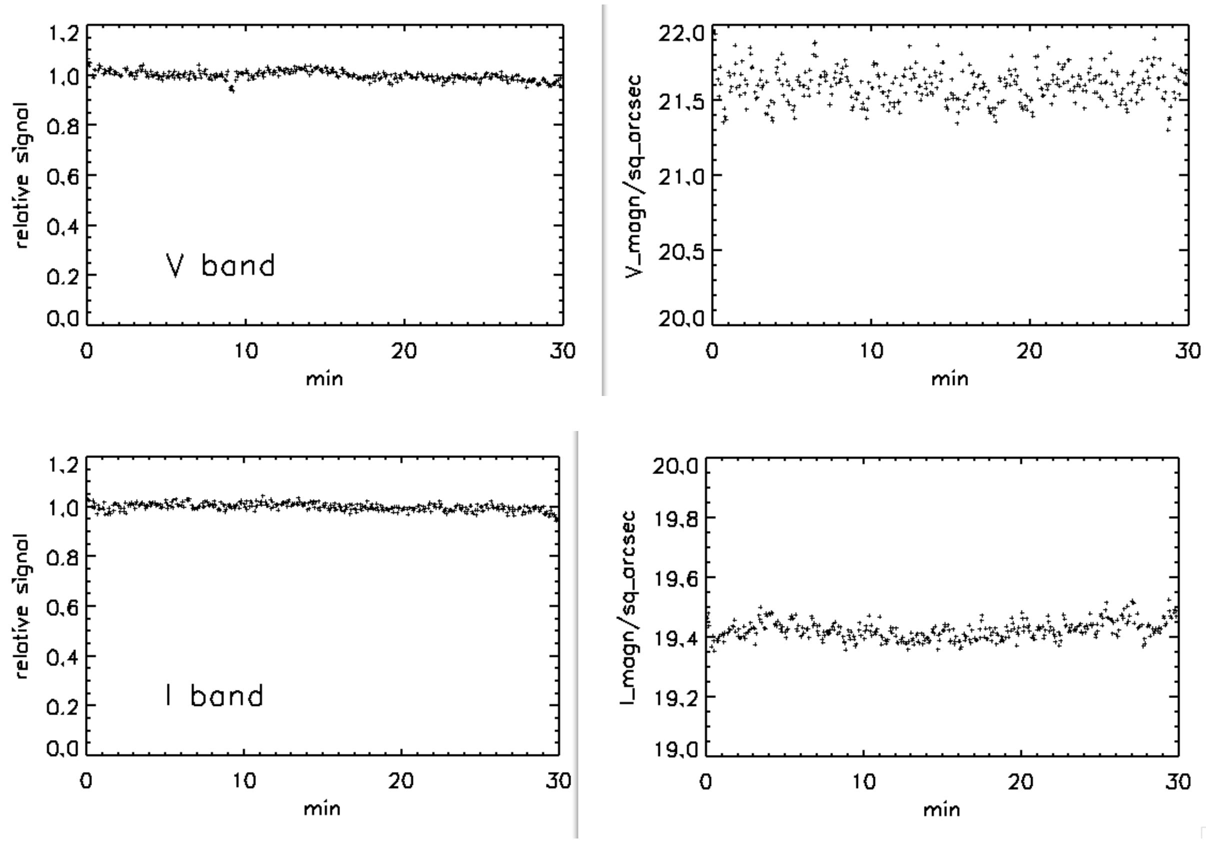

Fig 4. Both the sky transmission and emission were stable during the observations.

star observed directly after Mrk 900 and at the same air mass.

Results

The V and I images are shown in Fig 5 and in order to lower the noise we have smoothed slightly with a boxcar filter and in order to cope with the dynamics, the display is logarithmic. The FF corrections have been applied, and the sky emission has been subtracted (it is assumed that there is no halo emission in the NE and SE corners of the images).

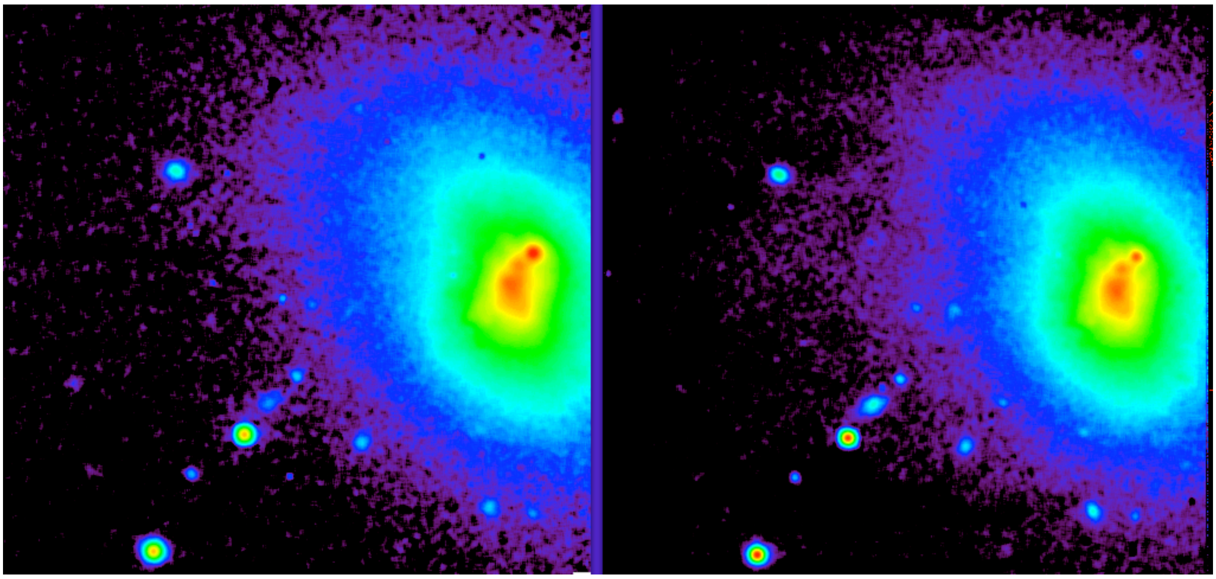

Fig 5 Mrk 900 in the V (left) and I (right) bands. In order to show the halo, a boxcar smoothing function with a width of 0.6 arcsec has been applied.

In Fig 6 we show the colour index $V-I$, constructed from the V and I images after convolution with a Gaussian (width = 1 arcsec). The halo is getting increasingly redder with projected distance from the centre of the galaxy, and it is noted that many of the red patches are in fact red background galaxies. These more or less point-like sources are most of them seen in Fig 5, and some additional appear in Fig 7 (where we have used a high-pass filter to remove the halo). In order to get the true colour of the

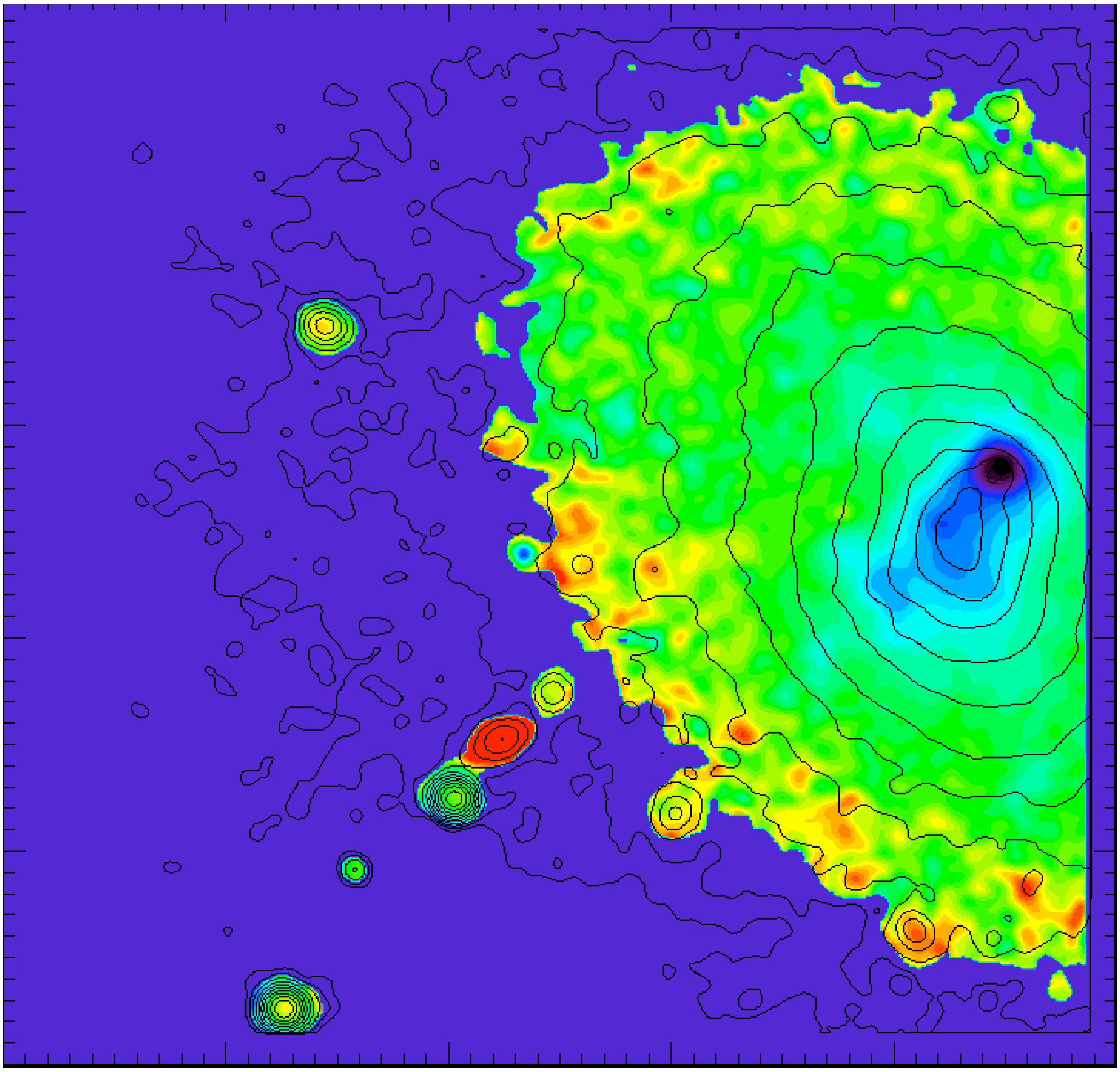

Fig 6 The colour index (V—I) where the colour code corresponds to <0.3 (black) and >1.4 (red). Regions with surface brightness less than V=24.1/sq_arcsec (i.e. 10% of the sky background) have been set at a constant value. The contour plot represents the sky brightness in the I band (0.5 magnitude steps).

halo as a function of the angular distance to the centre of Mrk 900, we have masked off the point sources. The result is shown in Fig 8, where we also show that the colour index V—I is *not* artificially altered by the differential PSFs. The method we have chosen for this test is simple: we have convolved the V and the I images with the respective PSFs. Thus, the observed images was (by definition) the result of the true images convolved with the PSFs. By convolving once more and comparing the resulting images with the observed we will, for low spatial frequencies, mimic the effect of the PSF smoothing of the original images. In view of the steep PSFs and small difference between that for V compared to that for I, we would not expect much colour effect of the extra convolution. This expectation is confirmed, as shown in Fig 8.

We conclude that, at least for PolCor-2, the PSF does not artificially make the halo of Mrk 900 red.

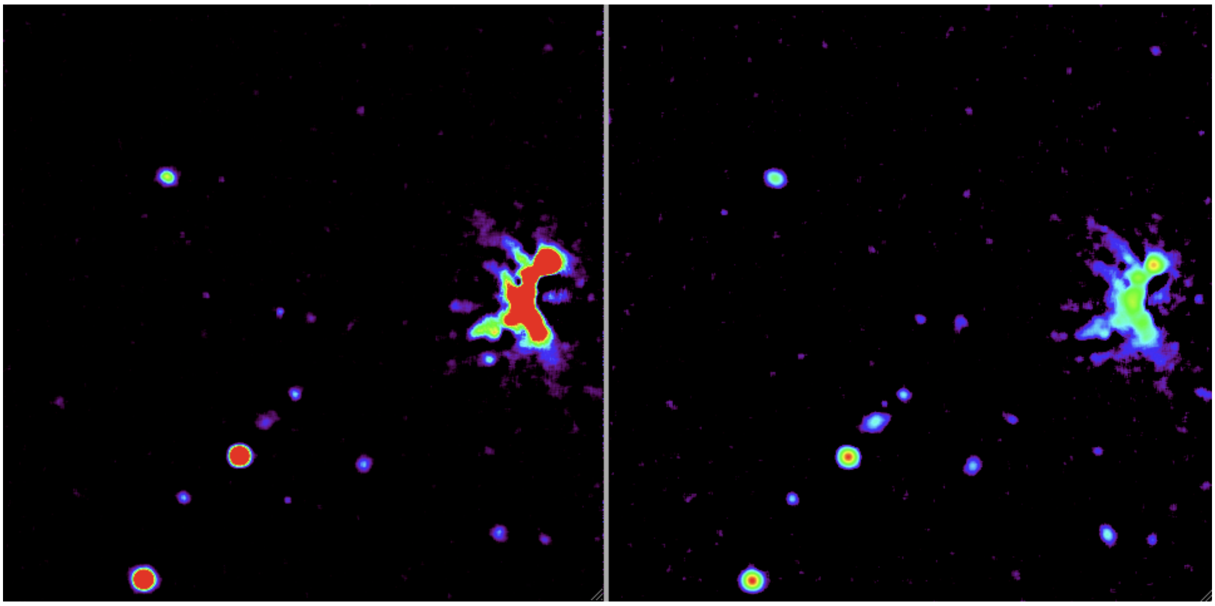

Fig 7 Mrk 900 high-pass filtered (left: V band and right: I band)

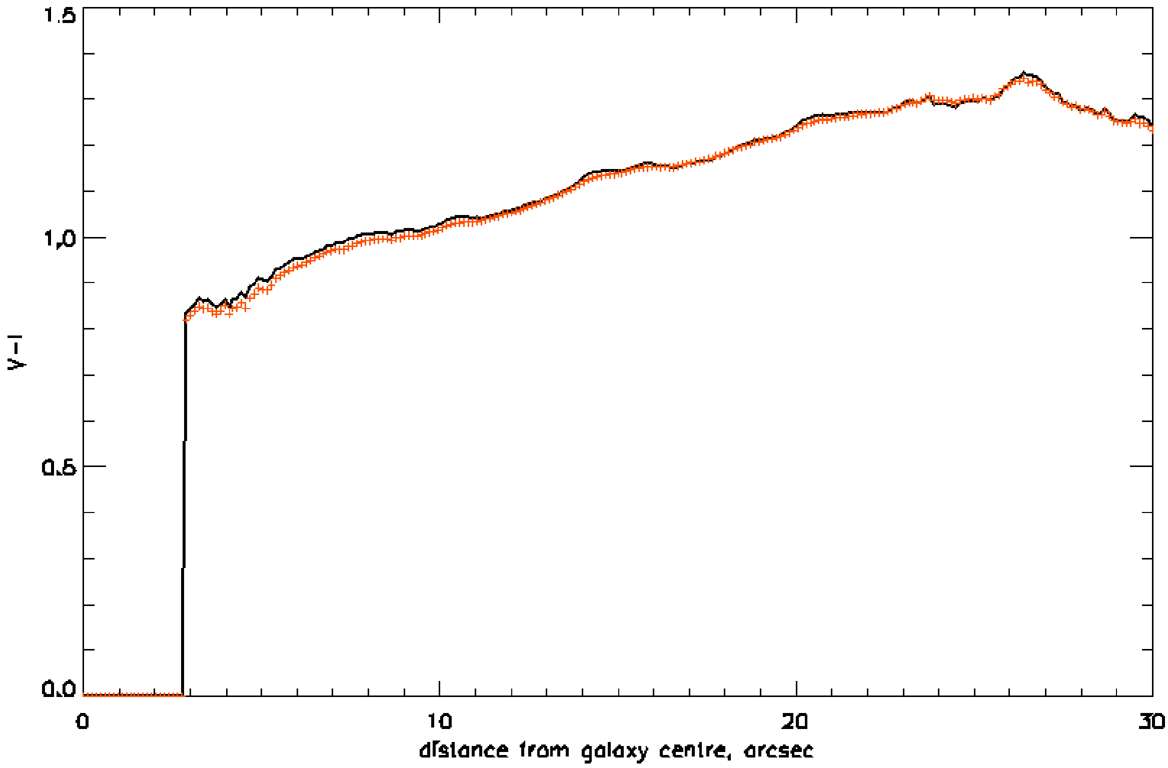

Fig 8 The V—I colour index as a function of the distance to the centre of Mrk 900. The limit for including halo points has here been set to V = 25 magn/sqarcsec. The decline of the curve at 27 arcsec may be an artifact. The black is as observed and the red is produced from images convolved with the respective PSFs. We note that such a 'doubling' of the PSF influence on the colour of the halo does not change the result, which implies that the PSF effect on the observed colour of the extended halo is negligible.

Concluding remarks

We have shown that the differential effect of the PSFs for an instrument like PolCor-2 on the measured V—I colour index of a typical (?) red halo around a blue, compact galaxy is marginal. It has, however, become clear that the usual worries about proper sky correction remain. The obvious way to solve this problem is the standard method used in the thermal infrared (where the sky is really bright compared to the targets), namely chopping and/or nodding. The noiseless (almost) readout of the EMCCD does allow short nodding cycles, and thereby accurate sky subtraction. This observing mode shall be implemented for PolCor-2.